Journal of Solid State Chemistry 181 (2008) 2837–2844

Contents lists available at ScienceDirect

Journal of Solid State Chemistry

journal homepage: www.elsevier.com/locate/jssc

Controlled drug release from bifunctionalized mesoporous silica

Wujun Xu [a,c], Qiang Gao [a,c], Yao Xu [a,*], Dong Wu [a], Yuhan Sun [a], Wanling Shen [b,c], Feng Deng [b]

[a] State Key Laboratory of Coal Conversion, Institute of Coal Chemistry, Chinese Academy of Sciences, Taiyuan 030001, PR China
[b] State Key Laboratory of Magnetic Resonance and Atomic and Molecular Physics, Wuhan Institute of Physics and Mathematics, Chinese Academy of Sciences, Wuhan 430071, PR China
[c] Graduate University of the Chinese Academy of Sciences, Beijing 100049, PR China

ARTICLE INFO

Article history:
Received 5 March 2008
Received in revised form
2 July 2008
Accepted 13 July 2008
Available online 20 July 2008

Keywords:
Mesoporous materials
Drug release
Famotidine

ABSTRACT

Serial of trimethylsilyl-carboxyl bifunctionalized SBA-15 (TMS/COOH/SBA-15) have been studied as carriers for controlled release of drug famotidine (Famo). To load Famo with large capacity, SBA-15 with high content of carboxyl groups was successfully synthesized by one-pot synthesis under the assistance of KCl. The mesostructure of carboxyl functionalized SBA-15 (COOH/SBA-15) could still be kept even though the content of carboxyl groups was up to 57.2%. Increasing carboxyl content could effectively enhance the loading capacity of Famo. Compared with pure SBA-15, into which Famo could be hardly adsorbed, the largest drug loading capacity of COOH/SBA-15 could achieve 396.9 mg/g. The release of Famo from mesoporous silica was studied in simulated intestine fluid (SIF, pH = 7.4). For COOH/SBA-15, the release rate of Famo decreased with narrowing pore size. After grafting TMS groups on the surface of COOH/SBA-15 with hexamethyldisilazane, the release of Famo was greatly delayed with the increasing content of TMS groups.

1. Introduction

In 2001, a new property of drug release based on mesoporous silica was disclosed by Vallet-Regi [1]. Subsequently, many groups have shown their interest in this new application of mesoporous silica [2–7]. It was found that drug loading and release rate could be well-adjusted by organic functionalization of mesoporous materials. Song et al. [2] found that aminopropyl-modified SBA-15 showed larger drug loading capacity than that of pure SBA-15 materials. In our group, it was observed that the release rate of ibuprofen could be obviously delayed by grafting trimethylsilyl (TMS) groups onto MCM-41 material [6]. Up to now, these achieved developments were mainly focused on single-organic-functionalized drug carriers. As we know, any kind of organic group possesses its distinct characteristic, and simultaneously has certain limitations. For example, hydrophobic alkyl groups could effectively reduce the release rate of ibuprofen, but these groups could not enhance its loading capacity of ibuprofen; though NH_2–Pr groups could enhance the loading capacity of ibuprofen, its reduction to the release rate of ibuprofen was worse than hydrophobic alkyl groups. Therefore, sometimes, single-functionalized mesoporous carriers were not able to meet the multiplicate demands of complicated human body.

Multi-functionalization should be a good method to make mesoporous silica possesses demanded multiplicate surface properties. New surface properties of mesopores could complement or promote with each other. Because of the confinement of mesopore structure, it is difficult to simultaneously functionalize three or more kinds of organic groups on the surface of mesoporous silica. Luckily, it was an easy thing to obtain bifunctionalized mesoporous silica materials, which have shown better behaviors than single-organic-functionalized materials in the fields of catalysis [8] and separation [9]. But, there were few reports about drug release system based on bifunctionalized mesoporous silica. Recently, Pasqua et al. [10] synthesized named "bifunctionalized" mesoporous silica for tumor-specific drug delivery by grafting aminopropyl group and folic acid on mesoporous silica. In this drug delivery system, the aminopropyl groups only acted as a bridge between mesoporous silica and folic acid, and it did not play a direct role in controlling drug loading capacity or drug release rate. So, though the mesoporous silica functionalized with two different groups, the obtained material did not possess true bifunctional properties. To some extent, the method should be a complex single-functionalization.

Famotidine (Famo) is a histamine H2-receptor antagonist for treatment ulcers in the stomach and intestine, whose molecule structure is presented in Fig. S1 (see supporting information). In 1985, Takabatake et al. [11] studied the pharmacokinetics of Famo and found its half-life of elimination was only 2.6 h in normal subjects. And later, Yeh et al. [12] found the bioavailability of oral

* Corresponding author. Fax: +86 351 4041153.
E-mail address: xuyao@sxicc.ac.cn (Y. Xu).

0022-4596/$ - see front matter © 2008 Elsevier Inc. All rights reserved.
doi:10.1016/j.jssc.2008.07.011

Famo (40 mg/times) just reached 43.0% and the blood concentration of Famo showed a severe peak-to-trough fluctuation. In order to void the disadvantages mentioned above, controlled release of Famo was developed for clinical application [13–15]. For example, Değim et al. [13] fabricated a biodegradable Famo microspheres of poly(lactide-*co*-glycolide) polymer by using multiple emulsion technique. It was found that the penetration of the Famo molecule could be controlled in this system, which might be useful for long-term treatments with Famo. Recently, the controlled release of Famo on inorganic porous materials was extended to mesoporous silica [16]. It was found that Famo could not be adsorbed into pure MSU, and the amount of Famo adsorbed into mesopores related with the surface COOH groups. However, there were still some unsolved problems in the system. In Ref. [16], the loading capacity of Famo was very low (only 160.4 mg/g), and it was unclear how the carboxyl groups affected the release rate of Famo. As we know, both of these questions were crucial for a drug release system. In order to further answer these questions, a novel TMS-carboxyl bifunctionalized drug release system was synthesized, in which these two kinds of organic groups complement with each other. To load Famo with large capacity, carboxyl groups were firstly functionalized on mesoporous SBA-15. Then TMS groups were grafted on the surface of mesoporous silica to control the release of Famo.

2. Experimental section

2.1. Preparation of carboxyl functionalized SBA-15 (COOH/SBA-15)

In a typical synthesis, 2-cyanopropyltriethoxysilane (CPTES) was introduced to HCl solution containing triblock copolymer Pluronic P123 ($EO_{20}PO_{70}EO_{20}$) and KCl. After hydrolyzed for 0.5 h under stirring at 40 °C, tetraethoxysilane (TEOS) was added into the mixture slowly. The molar composition of the mixture was (1.0−*x*) TEOS:*x* CPTES:0.015 P123:6.1 HCl:1.2 KCl:170 H_2O, where $x = 0$–0.50. Next, the resultant mixture was stirred at 40 °C for 20 h, followed by aging at 90 °C for 24 h under static condition. The solid product was recovered by filtration and dried at 60 °C. At last, according to the method of Yang et al. [17], the dried product was treated with 48.0% H_2SO_4 solution at 95 °C to eliminate the template and produce carboxyl functionalized SBA-15. Table 1 lists the detailed reactant compositions of the above samples.

2.2. TMS functionalization to COOH/SBA-15 after Famo loading

A total of 0.5 g dried COOH/SBA-15 and 0.75 g Famo were added to 500.0 mL mixed solvent of methanol and water (mass ratio of methanol:water = 0.8:1). After soaked for 8 h under stirring, the drug-loaded mesoporous powder was recovered by filtration. To measure the loading amount of Famo, 2.0 mL of filtrates was diluted to 50 mL and then analyzed using UV/Vis spectroscopy at the characteristic adsorption wavelength of Famo at 266.0 nm. Subsequently, the Famo-loaded samples were dried under vacuum at 50 °C for 24 h to remove residual solvent from obtained materials. The amount of Famo loaded in mesoporous silica was calculated by using

$$\text{wt\%} = \frac{m_1 - \frac{50}{v}CV}{m_2 + \left(m_1 - \frac{50}{v}CV\right)} 100\% \quad (1)$$

where m_1 and m_2 correspond to the initial mass of Famo and mesoporous silica added into the mixed solvent of water and methanol, respectively. C is the concentration of filtrates diluted in 50 mL volumetric flask, v is sampled volume from filtrates, and V is the volume of mixed solvent for drug loading.

Hexamethyldisilazane (HMDS) was used to silanize the drug-loaded COOH/SBA-15 in vapor phase. A 0.50 g drug-loaded C-15 sample was homogeneously spread on a piece of filter paper, which was put on a bracket in a beaker containing 1.0 mL HMDS. The beaker was closed and put in an oven at 50 °C. After determined treating time, the samples were taken out and dried under vacuum at 50 °C. These samples were designated as C-15M-A1 and C-15M-A2 corresponding to the different treating time of 0.5 and 3.0 h, respectively.

2.3. TMS functionalization to COOH/SBA-15 before Famo loading

In order to study the effect of silylation procedure on Famo loading and Famo release, the bifunctionalized SBA-15 was also prepared before Famo loading. A 0.50 g C-15 without loading drug was homogeneously spread on a piece of filter paper, which was put on a bracket in a beaker containing 1.0 mL HMDS. The beaker was closed and put in an oven at 50 °C. After determined treating time, the samples were taken out and dried under vacuum at 50 °C. The TMS-COOH bifunctionalized SBA-15 materials (TMS/COOH/SBA-15) were, respectively, assigned as C-15M-B1 and C-15M-B2 corresponding to the HMDS-treating time of 0.5 and 3.0 h.

The obtained TMS/COOH/SBA-15 samples were immersed into 500.0 mL mixed solvent of methanol and water to load Famo (mass ratio of methanol:water = 0.8:1). After soaked for 8 h, the drug-loaded mesoporous powder were recovered by filtration. To measure the loading amount of Famo, 2.0 mL of filtrates was diluted to 50 mL and then analyzed using UV/Vis spectroscopy. The loading amount of Famo was calculated based on Eq. (1).

2.4. In vitro drug release

The release profile of Famo was obtained by soaking drug-loaded powder in simulated intestine fluid (SIF, phosphate buffer solution, pH = 7.4). The release experiment was performed at 37 °C under stirring rate of 100 r/min. A 2.0 mL of release fluid was sampled at a predetermined time interval, and another 2.0 mL of fresh SIF was supplied immediately. The drug concentration in the sampled fluid was measured by UV–Vis spectrophotometer. Because some amount of Famo was sampled from the release fluid and this part of Famo could not be reflected in the latter sampling point. Therefore, a corrected method was used to calculate the actual amount of Famo released from mesoporous carriers. The calculation was based on the following equation [18]:

$$C_{t-\text{corr}} = C_t + \frac{v}{V}\sum_{0}^{t-1} C_t \quad (2)$$

where $C_{t-\text{corr}}$ is the actual concentration of Famo released at time t, C_t is the drug concentration in release fluid at time t measured on UV/Vis spectrometer, v is the sampled volume taken at a predetermined time interval, and V is the total volume of release fluid.

Table 1
The molar ratio of reactants for synthesis of carboxyl functionalized SBA-15

Sample	CPTES	TEOS	P123	KCl	$\frac{\text{CPTES}}{\text{CPTES+CPTES}}$
SBA-15	0.0	1.0	0.015	1.2	0.0
C-15	0.15	0.85	0.015	1.2	0.15
C-25	0.25	0.75	0.015	1.2	0.25
C-40	0.40	0.60	0.015	1.2	0.40
C-50	0.50	0.50	0.015	1.2	0.50

2.5. Materials characterizations

Powder XRD patterns were collected on a Rigaku diffractometer D8-Advance using Cu$K\alpha$ radiation. Nitrogen adsorption measurements were performed on a Micromeritics Tristar 3000 sorptometer at liquid nitrogen temperature. The specific surface area was calculated using the multiple-point Brunauer–Emmett–Teller (BET) method. The pore size distribution curve was calculated from the adsorption branch of the isotherm using the Barrett–Joyner–Halenda (BJH) method. The concentration of Famo in solution was measured on a Shimadzu UV-3150PC UV spectrometer. ^{29}Si MAS NMR experiments were performed on a Varian Infinityplus-300 spectrometer using 7.5 mm probe under magic-angle spinning: the resonance frequency was 79.5 MHz; the 90° pulse width was measured to be 4.8 μs; repetition time of 100 s for single-pulse experiments was used. The experiments for ^{13}C CP/MAS NMR were 2 s recycle delay, 20,000 scans, and 1 ms contact time.

3. Results

3.1. Characterization of functionalized SBA-15

Fig. 1 shows the powder XRD patterns of serial COOH/SBA-15 samples. For C-15 and C-25, there was a well-resolved peak and two small peaks that could be indexed to the diffraction (100), (110), and (200) due to the hexagonal array of SBA-15 mesopores. It could be seen that intensity of these peaks gradually decreased with the increasing content of organic groups. Notably, for sample C-50, there still existed a weak (100) peak at small angle region even though the molar ratio of CPTES/(TEOS+CPTES) was up to 0.50.

Fig. 2 shows the nitrogen ad/desorption isotherms of SBA-15 functionalized with different content of carboxyl groups. It could be seen that all samples exhibited a type IV isotherm that was the typical characteristic of mesoporous silica. With the increasing content of carboxyl groups, hysteresis loop of the isotherm was gradually changed. Samples C-15 (Fig. 2a) and C-25 (Fig. 2b) showed typical H1 hysteresis loop. But for samples C-40 (Fig. 2c) and C-50 (Fig. 2d), hysteresis loop of the isotherm was changed to H2-type. The change of hysteresis loop may be caused by the collapse of some mesopores, which was commonly found in the one-pot synthesized mesoporous silica containing organic groups in mesoporous framework [17,19]. In Fig. 2d, the type IV isotherm

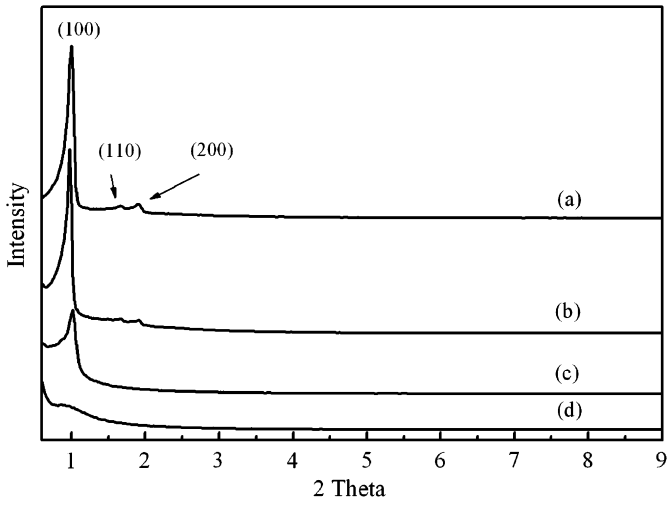

Fig. 1. XRD patterns of (a) C-15, (b) C-25, (c) C-40, and (d) C-50.

of C-50 could be still kept even though the molar ratio of CPTES/(TEOS+CPTES) was up to 0.50, confirming the XRD result. As shown in insets of Fig. 2(a–c), all COOH-functionalized silica exhibited narrow pore size distributions when CPTES/(CPTES+TEOS) was lower than 0.50. For sample C-50, the pore size distribution became wider a little. The textural parameters of mesoporous silica, including BET surface area (S_{BET}), pore volume (V_p), and pore size (D_p), are summarized in Table 2. These textural parameters were obviously affected by the introduction of carboxyl groups, all of these values decreased with the increasing content of carboxyl groups.

Solid-state ^{29}Si MAS NMR was used to provide information about silicon environment and the extent of organic functionalization. The ^{29}Si MAS NMR spectra of COOH/SBA-15 are presented in Fig. 3. Three resonances at −110, −101, and −92 ppm could be, respectively, assigned to Q^4, Q^3, and Q^2 species in the silica framework [$Q^n = Si(OSi)_n(OH)_{4-n}$, $n = 2–4$]. The two resonances at −65 and −55 ppm were, respectively, attributed to T^3 and T^2 [$T^m = COOH–Si(OSi)_m(OH)_{3-m}$, $m = 1–3$]. From Fig. 3, the signals assigned to *T*-band increased with the molar ratio of CPTES/(TEOS+CPTES). Interestingly, for samples C-40 and C-50, the total intensity of *T*-band signals was stronger than that of *Q*-band signals. The corresponding integral intensity of each resonance signal from ^{29}Si MAS NMR spectra are collected in Table 3. It was found that the content of carboxyl groups could be well controlled by adjusting the amount of CPTES. More noticeably, the content of carboxyl groups in C-50 sample could be high as 57.2%. So far, this value might be the highest organic functionalization extent that can be reached in mesoporous silica synthesized using only one kind of surfactant.

Fig. 4 shows the ^{29}Si MAS NMR spectra of serial TMS/COOH/SBA-15 samples, and their relative integral intensity are collected in Table 4. In Fig. 4, apart from the signals assigned to *T*-band and *Q*-band between −50 and −150 ppm, the new signal at 13.0 ppm could be attributed to TMS groups functionalized on the surface of mesoporous silica. It could be observed that the content of TMS groups on mesopores gradually increased with the silylation reaction time. For C-15M-A1 with silylation time of 0.5 h, the TMS content was about 9.8%. When the silylation time was prolonged from 0.5 to 3.0 h, the content of TMS groups increased to 14.1%. This changed trend also existed in samples C-15M-B1 and C-15M-B2, that is, when the silylation reaction time increased from 0.5 to 3.0 h, TMS content increased from 10.9% to 15.4%.

According to Daehler's method [20], the ^{29}Si MAS NMR data shown in Tables 3 and 4 could be used to calculate the concentrations of carboxyl groups and TMS groups contained in functionalized SBA-15, based on the following equations:

$$[\mathrm{COOH}] = \frac{\%T^2 + \%T^3}{\sum(\%Q^n \times \mathrm{EMW}_{Q^n}) + \sum(\%T^m \times \mathrm{EMW}_{T^m})} \times 1000 \quad (3)$$

$$[\mathrm{TMS}] = \frac{\%M}{\sum(\%Q^n \times \mathrm{EMW}_{Q^n}) + \sum(\%T^m \times \mathrm{EMW}_{T^m}) + \sum(\%M \times \mathrm{EMW}_M)} \times 1000 \quad (4)$$

where [COOH] and [TMS], respectively, correspond to the COOH concentration and TMS concentration with mmol/g as unit; $\%Q^n$, $\%T^m$, and $\%M$, respectively, correspond to the relative integral intensity of *Q*, *T*, and *M* species in ^{29}Si MAS NMR; EMW is the effective molar weight of the attached groups. For example, the EMW value of Q^2 is 78 based on the structure of $SiO(OH)_2$. The calculated [COOH] and [TMS] were respectively shown in Tables 2 and 4. It could be seen that the [COOH] increased with CPTES/(CPTES+TEOS) and [TMS] increased with silylation reaction time.

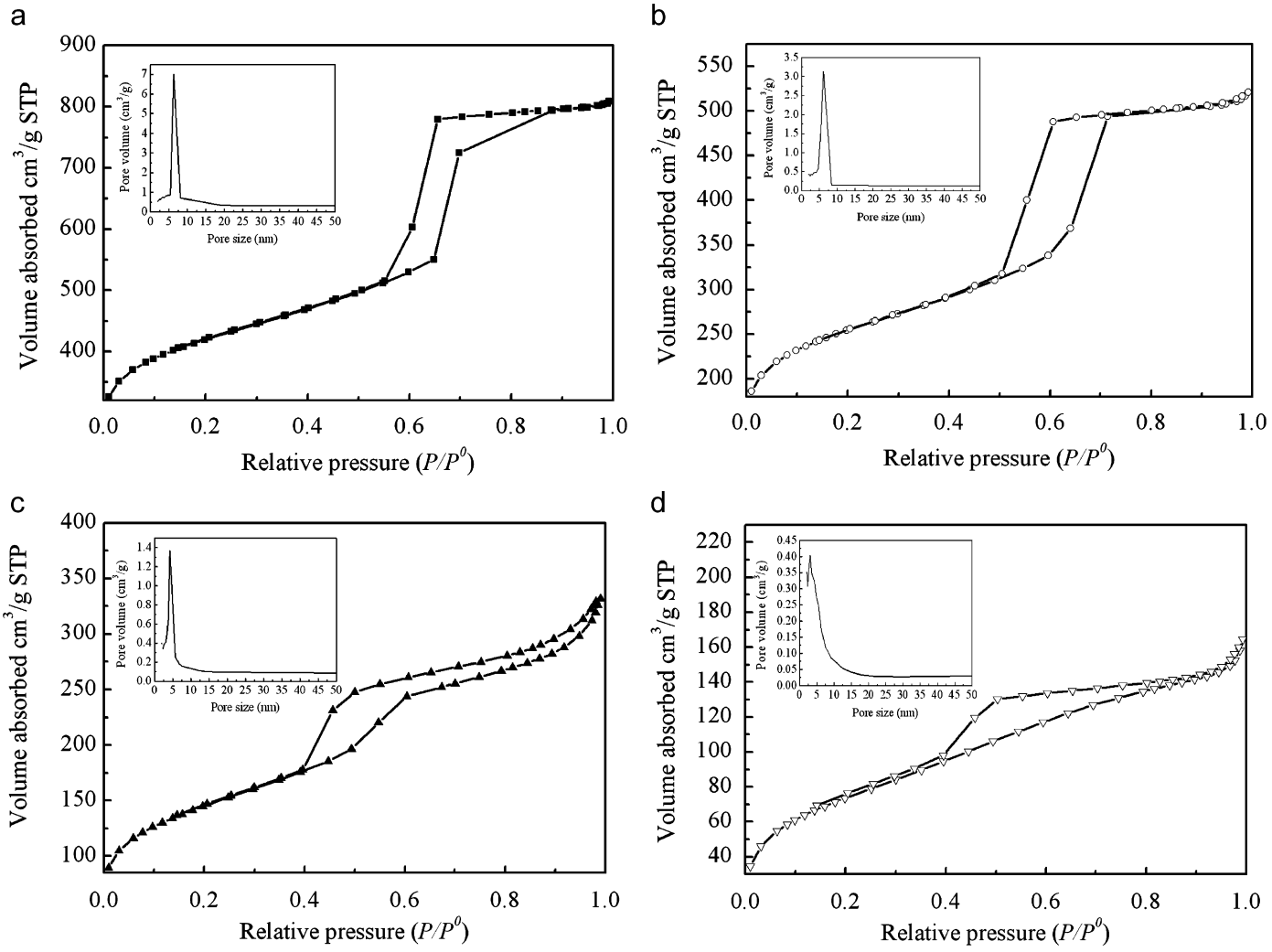

Fig. 2. BET isotherms and BJH pore size distributions (inserts) patterns of (a) C-15, (b) C-25, (c) C-40, and (d) C-50.

Table 2
Structure information and Famo loading capacity of carboxyl functionalized SBA-15

Sample	S_{BET} (m^2/g)	V_p (cm^3/g)	D_p (nm)	[COOH][a] (mmol/g)	Famo loading (mg/g)
SBA-15	887.1	1.157	7.5	0.0	–
C-15	633.9	0.864	6.3	2.0	250.0
C-25	450.0	0.597	6.1	3.4	337.9
C-40	359.0	0.436	4.2	4.8	396.9
C-50	272.3	0.255	3.1	5.4	233.2

[a] Carboxyl group concentration.

3.2. Drug loading

Tables 2 and 4 also list the drug loading capacity of COOH/SBA-15 and TMS/COOH/SBA-15. In Table 2, it could be found that Famo loading capacity was directly related to the content of carboxyl groups in mesoporous silica. For pure SBA-15, Famo molecules could be hardly adsorbed into mesopores, which was consistent with the previous report [16]. After functionalized with carboxyl groups, the Famo loading capacity was greatly enhanced. For C-15 with 2.0 mmol/g carboxyl groups, its Famo loading capacity quickly reached 250.0 mg/g. When [COOH] increased from 2.0 mmol/g of C-15 to 4.8 mmol/g of C-40, the Famo loading capacity of COOH/SBA-15 was enhanced from 250.0 to 396.9 mg/g. But, if the [COOH] further increased to 5.4 mmol/g of C-50, the Famo loading capacity decreased to 233.2 mg/g again.

To study the effect of TMS groups on Famo loading, different silylation procedures were used. For samples C-15M-A1 and C-15M-A2, because the Famo loading has been accomplished before TMS silylation, the loading capacity of Famo was independent of silylation reaction. But for samples C-15M-B1 and C-15M-B2, after grafted TMS groups on the surface of COOH/SBA-15, their Famo loading capacity decreased with the increase of TMS content (see Table 4). Especially, for C-15M-B2 with 2.3 mmol/g [TMS], only 63.8 mg/g Famo could be loaded into bifunctionalized SBA-15. Therefore, in practical application, to ensure enough amount of drug to be loaded into mesoporous carrier, it is necessary to load drug before TMS silylation.

IR spectra of pure SBA-15, C-15 and Famo-loaded C-15 are shown in Fig. 5 to identify the interaction between Famo molecules and carboxyl functionalized SBA-15. In the three spectra, the peaks shown at 1630 and 1410 cm^{-1} could be attributed to H_2O adsorbed in mesopores. Compared with blank pure SBA-15 (Fig. 5a), the peak at 1718 cm^{-1} in the spectrum of C-15 (Fig. 5b) was attributed to the stretching vibration of C=O in COOH group. And no vibration of the original –CN groups introduced by CPTES could be found at 2250 cm^{-1}, indicating that

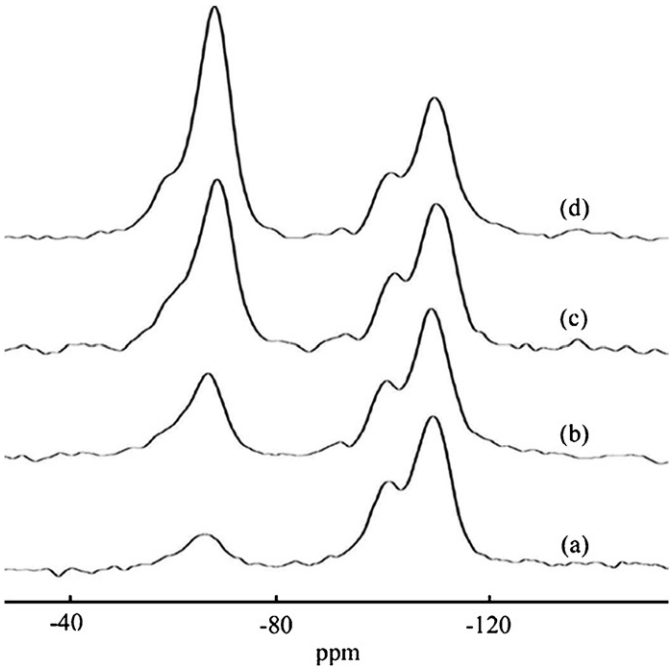

Fig. 3. ^{29}Si MAS NMR spectra of carboxyl functionalized SBA-15: (a) C-15, (b) C-25, (c) C-40, and (d) C-50.

Table 3
^{29}Si MAS NMR data of carboxyl functionalized SBA-15

Sample	Relative integral intensity (%)					COOH content (%)[a]
	Q^4	Q^3	Q^2	T^3	T^2	
C-15	55.9	29.0	0.8	14.3	–	14.3
C-25	59.6	10.9	0.9	18.1	10.5	28.6
C-40	37.9	12.2	1.0	35.9	13.0	48.9
C-50	36.7	6.1	-	46.5	10.7	57.2

[a] Obtained from $T^m/(T^m+Q^n)$, $T^m = T^3+T^2$, $Q^n = Q^4+Q^3+Q^2$.

all of the –CN groups have been hydrolyzed into COOH groups through H_2SO_4 treatment. An intense carboxylate vibration appeared at 1550 cm^{-1} in the IR spectrum of drug-loaded C-15, proving that the proton transfer indeed took place from carboxyl groups on mesopore surface to amino groups of Famo molecules (Fig. 5c).

3.3. Drug release

In vitro release experiments were employed to evaluate drug release rate of these bifunctionalized mesoporous SBA-15, and the Famo-loaded mesoporous powder was directly used in the release experiments. Fig. 6 showed the released percentage of Famo as a function of time for COOH/SBA-15 in SIF. Under stirring at a rate of 100 r/min, Famo release from COOH/SBA-15 shows similarly burst release within the first hour, during which 95.0, 94.0, 74.4, and 88.0 wt% Famo was, respectively, released from C-15, C-25, C-40, and C-50. As shown in Fig. 6, though C-25 had obviously higher [COOH] than that of C-15, their drug release profiles were very similar with each other. Due to smaller pore size, the Famo release from samples C-40 and C-50 were delayed. But for C-50, because its collapsed pores reduced the structure orderness of mesoporous silica, the release of Famo from C-50 became faster than that from C-40.

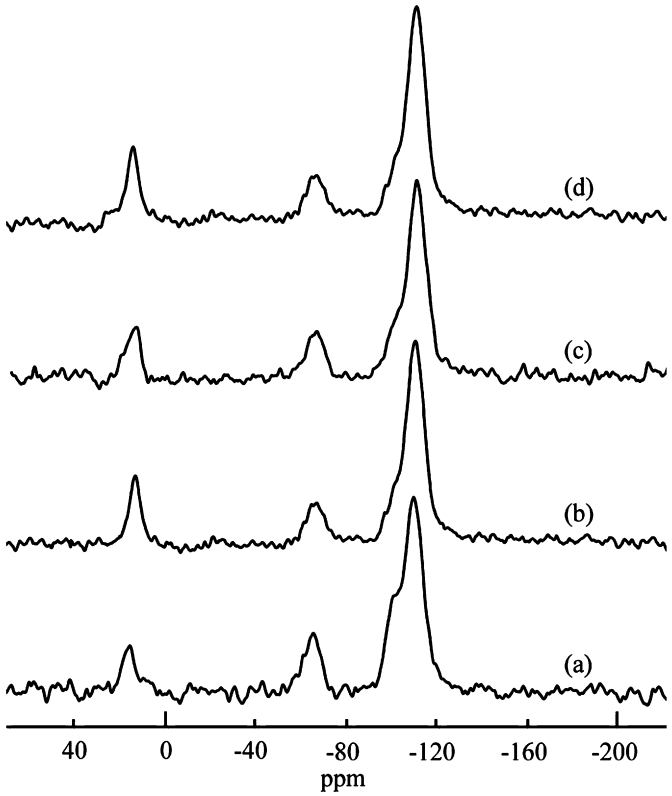

Fig. 4. ^{29}Si MAS NMR spectra of TMS-carboxyl bifunctionalized SBA-15: (a) C-15M-A1, (b) C-15M-A2, (c) C-15M-B1, and (d) C-15M-B2.

Table 4
^{29}Si MAS NMR data and Famo loading capacity of TMS-carboxyl bifunctionalized SBA-15

Sample	Relative integral intensity (%)					[TMS][a] (mmol/g)	Famo loading (mg/g)
	Q^4	Q^3	Q^2	T^3	M		
C-15M-A1	56.7	18.7	0.7	14.1	9.8	1.5	250.0
C-15M-A2	57.8	14.2	0.6	13.3	14.1	2.1	250.0
C-15M-B1	57.0	17.6	0.7	13.8	10.9	1.6	140.3
C-15M-B2	58.3	12.7	0.4	13.2	15.4	2.3	63.8

[a] TMS group concentration.

Fig. 7 shows the release profiles of Famo from serial TMS/COOH/SBA-15 samples. For the samples synthesized by same silylation procedure, the release rate of Famo from bifunctionalized SBA-15 decreased with the increasing [TMS]. Compared with C-15, though the full release time for C-15M-A1 was only 6.0 h, the amount of Famo released from C-15M-A1 (with 1.5 mmol/g TMS groups) decreased to 88.4 wt% within the first hour. For C-15M-A2 (with 2.1 mmol/g TMS groups), the burst release phenomenon of Famo disappeared on the whole: only 31.3 wt% Famo was released from the carrier within the first hour. When the time was up to 10.0 h, the Famo release amount from C-15M-A2 just reached 80.0 wt%. Similarly, due to more TMS groups on the surface of C-15M-B2, Famo release from C-15M-B2 was also slower than that from C-15M-B1. Even though the burst release phenomenon of Famo did not disappear in samples C-15M-B1 and C-15M-B2, but underwent a little weakening. During the first hour, there were 92.0 and 69.0 wt% of Famo released from C-15M-B1 and C-15M-B2, respectively. Furthermore, if we drew a comparison between C-15M-A1 and C-15M-B1, or between C-15M-A2 and C-15M-B2, it

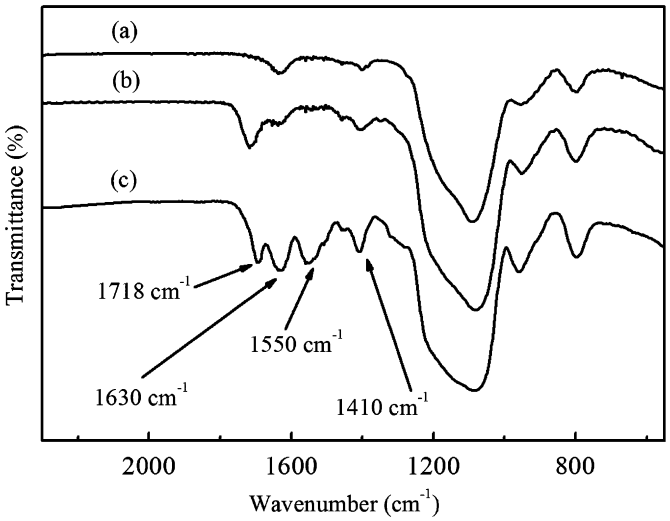

Fig. 5. FT-IR spectra of (a) SBA-15, (b) C-15, and (c) drug-loaded C-15.

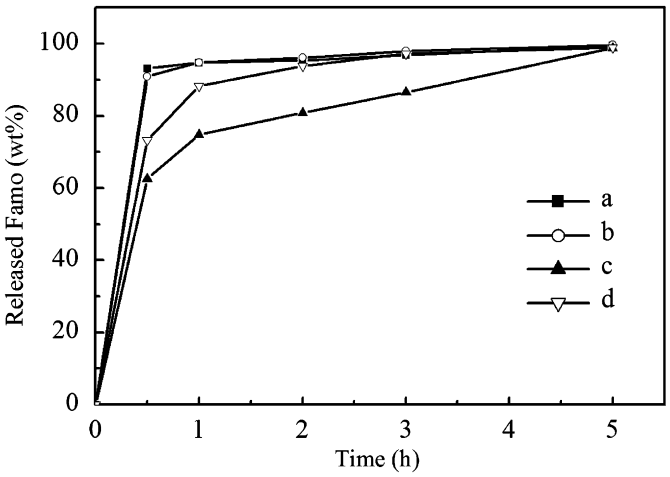

Fig. 6. Release profiles of Famo from COOH/SBA-15 in SIF: (a) C-15, (b) C-25, (c) C-40, and (d) C-50.

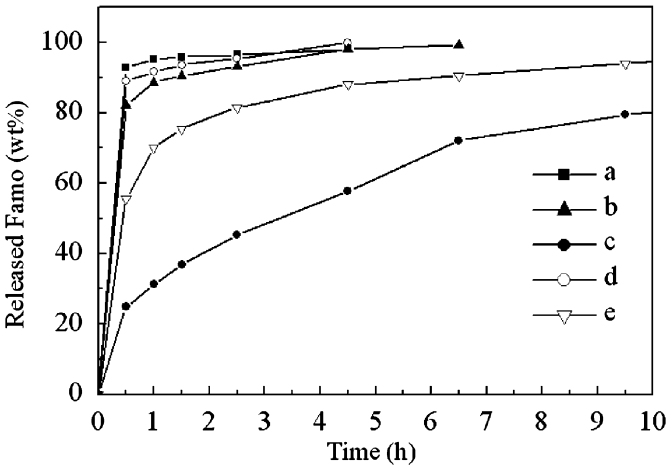

Fig. 7. Release profiles of Famo from TMS/COOH/SBA-15 in SIF: (a) C-15, (b) C-15M-A1, (c) C-15M-A2, (d) C-15M-B1, and (e) C-15M-B2.

could be found that the mesoporous silica grafted with TMS groups after Famo loading possessed slower Famo release rate. Though [TMS] of C-15-B1 and C-15M-B2 was only slightly higher, respectively, than that of C-15M-A1 and C-15M-A2, the release rates of Famo from C-15-B1 and C-15M-B2 were far more faster than the coupling two samples. For C-15M-B2, more than 95.0 wt% Famo was released within 10.0 h. But, at the same time interval, there was only 80.0 wt% Famo was released from C-15M-A2.

4. Discussion

4.1. Synthesis of SBA-15 with high carboxyl content

The first aim of this work was to obtain a drug carrier possessing a large loading capacity of Famo because Famo could hardly be loaded into pure SBA-15. Based on the finding that the Famo loading capacity was related to the content of carboxyl groups, mesoporous SBA-15 should be functionalized with carboxyl groups as many as possible. But, generally, because of the different hydrolysis and condensation rate between organosiloxane and TEOS, it was very difficult to synthesize mesoporous silica with more than 30% (molar ratio) organic groups by one-pot method. So, synthesis of mesoporous silica with higher content of organic groups was a challenge. Some important progresses in this aspect have been made during the past several years. Feng et al. [21] synthesized HS-JLU-20 with 50–80% (molar ratio) of mercaptopropyl groups using a surfactant mixture of fluorocarbon surfactant (FC-4) and block copolymer (P123). However, because surfactant FC-4 was not biocompatible and there were more or less residual FC-4 in mesopores after surfactant extraction, the obtained materials were unsuitable to be used in drug release system. Wang et al. [22] obtained vinyl functionalized SBA-15 with 40% (molar ratio) of organic groups under the assistance of $MgCl_2$. After reaction, $MgCl_2$ could be easily eliminated from products by water washing.

In this paper, inorganic salt KCl was used as additive to synthesize carboxyl functionalized SBA-15. To study the effect of KCl on the structure of COOH/SBA-15, two samples were synthesized without adding KCl. The detailed reactant compositions were shown in supporting information, and the obtained materials were characterized by XRD. It could be found that the degree of structure orderness of product was obviously increased after adding KCl in the reaction system (see supporting information, Fig. S2). Under the effect of KCl, the obtained COOH/SBA-15 possessed fiber-like morphology with the length range from 20 to 100 μm (see supporting information, Fig. S3) [23]. With the increase of carboxyl content, the regularity of fibers decreased and the length of these fibers was shortened. This phenomenon might be also caused by the different hydrolysis and condensation rate between CPTES and TEOS.

As for the contribution of KCl to the orderness of pore arrange, the existence of KCl might favor the interactions between surfactant micelles and the oligomers of siloxane [24]. In aqueous solution, P123 molecules formed micelles with cores of PPO blocks surrounded by shells of hydrated PEO blocks. After KCl was dissolved in the solution, the hydrophobicity of PEO blocks increased and the hydrophilicity of PPO blocks reduced [25], which promoted the interactions between PEO headgroups and organosiloxane species with relatively weak hydrophilicity [26]. This enhanced interface interactions resulted in a more ordered mesostructure of carboxyl functionalized SBA-15.

4.2. Surface silylation of COOH/SBA-15

Previous researches have systematically investigated the reactive activity of different kinds of Si–OH groups [27–30]. Only

isolated Si–OH groups, including free and geminal Si–OH, were active sites to react with HMDS. The reaction between HMDS and Si–OH could be expressed as [31]

$$2Si-OH + HN(Si(CH_3)_3)_2 \rightarrow 2Si-O-Si(CH_3)_3 + NH_3 \quad (5)$$

According to the foregoing results, drug adsorption could be attributed to the interaction between the carboxyl groups on mesoporous silica and the amino groups of Famo. But, Famo molecules could not occupy all carboxyl groups, and the peak at 1718 cm^{-1} in Fig. 5c confirmed that there still existed some free carboxyl groups on the pore surface of drug-loaded COOH/SBA-15. Considering that Si–OH groups and COOH groups coexisted on the surface of COOH/SBA-15, it was a crucial question whether there was a competition between Si–OH group and COOH group to react with HMDS. If COOH groups could react with HMDS, the reaction must follow below equation:

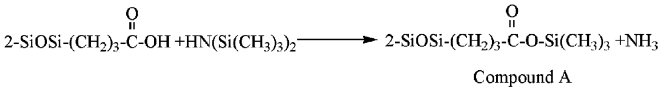

(6)

Thus, a new compound A must be produced on the surface of TMS/COOH/SBA-15. However, no evidence of compound A could be found from the ^{29}Si MAS NMR results shown in Fig. 4. In order to confirm this result, newly synthesized COOH/SBA-15 (C-15) was subjected to be treated with HMDS. Then, ^{13}C CP/MAS NMR and FT-IR were employed to provide direct evidences for the impossibility of reaction (6). Fig. 8 shows the ^{13}C CP/MAS NMR spectra of carboxyl functionalized SBA-15 (C-15) and TMS-carboxyl bifunctionalized SBA-15 (C-15M-B2 without drug). For C-15, the resonance at 178.8 ppm was attributed to the C atom (no. 1) of COOH group [17]. The resonance peaks at 37.5, 19.3, and 12.8 ppm were, respectively, corresponding to the nos. 2, 3, and 4 C atoms in the carbon chain of $-(CH_2)_3-COOH$. After treatment with HMDS, only one new peak appeared at 1.0 ppm and should be assigned to the C atom (no. 5) of CH_3 in TMS groups. Compared with C-15, the resonance of no. 1 C atom (178.8 ppm) of C-15M-B2 did not change at all. If HMDS molecules can react with COOH groups, the resonance of no. 1 C atom must be divided into two peaks: one is for COOH and another is for $COOSi(CH_3)_3$. The IR spectra of carboxyl functionalized SBA-15 (C-15) and TMS-carboxyl bifunctionalized SBA-15 (C-15M-B2 without drug) are shown in Fig. 9. In Fig. 9b, the TMS group could be easily recognized by the peak at 1257 cm^{-1} accompanied by two

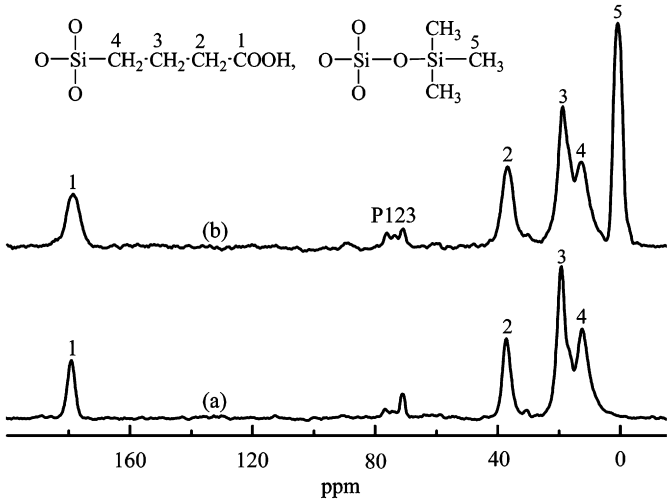

Fig. 8. ^{13}C CP/MAS NMR spectra of (a) C-15 and (b) C-15M-B2 without drug loading.

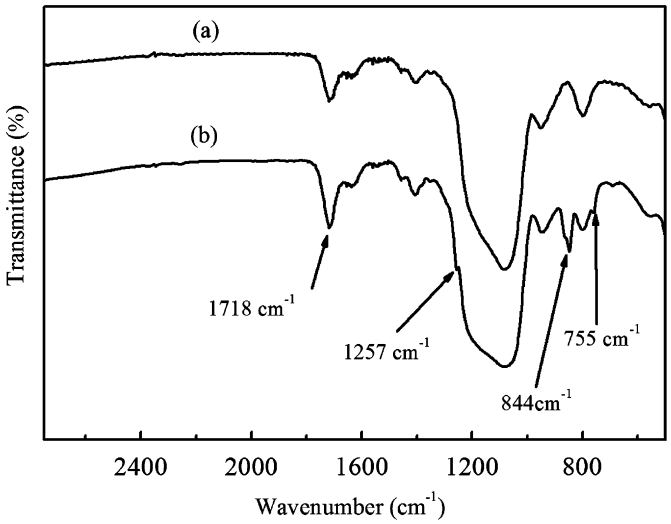

Fig. 9. FT-IR spectra of (a) C-15 and (b) C-15M-B2 without drug loading.

peaks at 844 and 755 cm^{-1} that was came from the $-CH_3$ rocking and the Si–C stretching vibrations [32]. No vibration of carboxylate at 1550 cm^{-1} could be found in Fig. 9b confirming the result obtained from ^{29}Si MAS NMR and ^{13}C CP/MAS NMR spectra.

As we know, the electronegativity of carbon ($x_C = 2.55$) was higher than that of silicon ($x_{Si} = 1.90$). Moreover, C atom in the COOH groups was of sp^2 hybridization, while Si atom in SiOH was of sp^3 hybridization. As a result, the electron cloud density of O in SiOH was obviously larger than that of O in OH connected with C=O. Therefore, in the nucleophilic substitution reaction of HMDS with OH groups, the OH in SiOH groups were more active than that in COOH groups, determining that the reaction (6) could not proceed.

4.3. Effects of carboxyl and TMS groups on drug loading

As shown in Table 2, through synthesis of mesoporous silica with high content of carboxyl groups, large drug loading capacity was successfully achieved, and the Famo loading capacity could be well regulated. In our previous work, the adsorption of Famo was studied in methanol and methanol–water mixed solvent [33]. The solubility of Famo in methanol was larger than that in water. It was very slightly soluble in water. So, in methanol–water mixed solvent, the addition of water reduced the interaction between Famo and methanol [34], resulting in an enhancement of drug loading capacity. In other words, high solubility of the organic molecule in the solvent would work against the adsorption to the interface. Therefore, the adsorption experiment in this report was processed in the methanol–water mixed solvent.

To discuss the effect of carboxyl groups on Famo loading, it should be firstly noted that the COOH content derived from NMR studies typically gave the total content of groups, not the number of accessible groups for Famo loading. According to Rosenholm's report [35], only about 30% of the COOH groups were accessible for the adsorption of Famo. From Table 2, it was found this corresponded well to the amount of Famo adsorbed into the COOH/SBA-15. There was almost a 1:1 adsorption of Famo to the accessible COOH groups. With increasing content of carboxyl content, the Famo loading amount also increased. For C-40, considering the Famo molecule size ($1.7862 \times 0.5329 \times 1.8307$ nm) [16], some of surface carboxyl groups could not be utilized to adsorb Famo molecules because of the shielding effect of Famo molecules. Thus, the Famo loading amount of C-40 in our experiment was a little smaller than that calculated from Rosenholm's method. For C-50, collapse of some pore channels caused the decrease of Famo loading.

Compared with C-15, the Famo loading capacity of bifunctionalized C-15M-B1 and C-15M-B2 decreased obviously (see Table 4), which resulted from the increase of surface hydrophobicity by grafting TMS groups. As we know, Famo is a hydrophilic drug [36]. Therefore, increasing the surface hydrophobicity of mesoporous materials was unfavorable for loading Famo [37]. Qu et al. [4] also found the similar phenomenon when they studied the adsorption of hydrophilic drug Captopril in TMS functionalized MCM-41. Thus, with the increasing content of TMS groups, the Famo loading capacity of C-15M-B2 decreased to 63.8 mg/g.

4.4. Effects of carboxyl and TMS groups on drug release

Because of the different hydrolysis and condensation rate between TEOS and CPTES, some mesopores were imperfectly constructed if a lot of carboxyl groups were introduced, which could lead to the decrease of pore size, surface area and pore volume. As for the effect of pore structure on drug release rate, several previous reports have proved that narrowing pore size could delay the drug release from mesoporous carriers [33,38]. Based on the results shown in Table 2, the pore size of COOH/SBA-15 samples decreased with the increasing content of carboxyl groups. Thus, the release of Famo from C-40 and C-50 was slower than that from C-15 and C-25. Similarly, because the difference of pore size between C-15 (6.3 nm) and C-25 (6.1 nm) was only 0.2 nm, their release profiles were very close with each other despite of higher [COOH] of C-25 than that of C-15. These results indicated that the release rate of Famo in COOH/SBA-15 was influenced mainly by the pore size, not by the content of COOH groups. In COOH/SBA-15, active sites for Famo adsorption were surface COOH groups, not Si–OH groups. The increasing carboxyl content on surface of mesoporous silica could not change the interaction type between Famo molecules and carboxyl groups, and only enhanced the number of active sites for drug adsorption. Therefore, if the carboxyl functionalized mesoporous silica possessed similar pore size, the increasing content of carboxyl groups would not affect obviously the rate of Famo release.

As we know, as a good drug release system, besides large drug loading capacity, drug release rate must be well controlled. So, for COOH/SBA-15 with high Famo loading amount, their drug release controllability became the second problem that must be taken into account. TMS surface silylation was employed to adjust the release rate of Famo from COOH/SBA-15. Among the four COOH/SBA-15 samples, C-15 possessed the most ordered mesopore structure. The release profiles obtained from bifunctionalized C-15 were more representative. Therefore, C-15 was chosen as a model carrier to synthesize bifunctionalized drug carriers. As shown in Fig. 7, drug release could be effectively controlled by TMS groups functionalized on the surface of mesoporous silica. Because its strong hydrophobic property, TMS groups could delay the release fluid to penetrate into the mesopore channels and hence delay the Famo molecules to move out of the mesopore channels [4,6]. From the release profiles of C-15M-A1, C-15MA2, C-15M-B1 or C-15M-B2, the delay effect of TMS groups was found to be enhanced with the content of TMS groups. For samples C-15M-A1 and C-15M-A2, because the adsorbed Famo molecules shielded part of Si–OH on the surface of mesoporous silica, there should be more TMS groups functionalized on the pore openings. Besides its hydrophobic property, the TMS groups on the pore openings could act as "barrier" to delay the release of Famo.

5. Conclusion

Under the assistance of KCl, SBA-15 with high content of carboxyl groups was successfully one-pot synthesized using surfactant P123. The loading capacity of Famo could be well controlled by regulating the content of carboxyl groups. Through post-treating drug-loaded COOH/SBA-15 with HMDS, a well-controlled Famo release can be achieved.

Acknowledgments

The financial support from the National Native Science Foundation (no. 20573128), Shanxi Native Science Foundations (nos. 20051025 and 2006021031) were acknowledged.

Appendix A. Supplementary Materials

Supplementary data associated with this article can be found in the online version at doi:10.1016/j.jssc.2008.07.011.

References

[1] M. Vallet-Regi, A. Ramila, R.P. del Real, J. Perez-Pariente, Chem. Mater. 13 (2001) 308–311.
[2] S.W. Song, K. Hidajat, S. Kawi, Langmuir 21 (2005) 9568–9575.
[3] B. Munoz, A. Ramila, J. Perez-Pariente, I. Diaz, M. Vallet-Regi, Chem. Mater. 15 (2003) 500–503.
[4] F.Y. Qu, G.S. Zhu, S.Y. Huang, S.G. Li, et al., Chemphyschem 7 (2006) 400–406.
[5] J.C. Doadrio, E. Sousa, I. Izquierdo-Barba, A.L. Doadrio, J. Perez-Pariente, M. Vallet-Regi, J. Mater. Chem. 16 (2006) 462–466.
[6] Q.L. Tang, Y. Xu, D. Wu, Y.H. Sun, J. Wang, J. Xu, F. Deng, J. Control. Rel. 114 (2006) 41–46.
[7] Nigel W. Clifford, K. Swaminathan Iyer, C.L. Raston, J. Mater. Chem. 18 (2008) 162–165.
[8] Ryan K. Zeidan, M.E. Davis, J. Catal. 247 (2007) 379–382.
[9] G. Zhu, Q. Yang, D. Jiang, J. Yang, L. Zhang, Y. Li, C. Li, J. Chromatogr. A 1103 (2006) 257–264.
[10] L. Pasqua, F. Testa, R. Aiello, S. Cundari, J.B. Nagy, Micropor. Mesopor. Mater. 103 (2007) 166–173.
[11] T. Takabatake, H. Ohta, M. Maekawa, Y. Yamamoto, Y. Ishida, H. Hara, Eur. J. Clin. Pharmacol. 28 (1985) 327–331.
[12] K.C. Yeh, A.N. Chremos, J.H. Lin, M.L. Constanzer, S.M. Kanovsky, H.B. Hucker, J. Antonello, P. Vlasses, J.R. Ryan, R.L. Williams, Biopharm. Drug Dispos. 8 (1987) 549–560.
[13] Z. Değim, N. Unal, D. Essiz, U. Abbasoğlu, Drug Deliv. 12 (2005) 27–33.
[14] P. He, S.S. Davis, L. Illum, J. Microencapsulation 16 (1999) 343–355.
[15] H.X. Zeng, W.S. Pan, J.M. Chen, Chin. Pharm. J. 3 (1997) 213–216.
[16] Q. Tang, Y. Xu, D. Wu, Y. Sun, J. Solid State Chem. 179 (2006) 1512–1519.
[17] C. Yang, Y. Wang, B. Zibrowius, F. Schuth, Phys. Chem. Chem. Phys. 6 (2004) 2461–2467.
[18] K.A. Fisher, K.D. Huddersman, M. Taylor, J. Chem. Eur. J. 9 (2003) 5873–5878.
[19] S.M. Chong, X.S. Zhao, T. Angeline, S.Z. Qiao, Micropor. Mesopor. Mater. 72 (2004) 33–42.
[20] A. Daehler, S. Boskovic, M.L. Gee, F. Separovic, G.W. Stevens, A.J. O'Connor, J. Phys. Chem. B 109 (2005) 16263–16271.
[21] Y. Feng, Y. Di, Y. Du, Y. Zhang, F. Xiao, J. Phys. Chem. B. 110 (2006) 14142–14147.
[22] Y. Wang, C. Yang, B. Spliethoff, F. Schüth, Chem. Commun. 1 (2004) 46–47.
[23] K. Kosuge, T. Sato, N. Kikukawa, M. Takemori, Chem. Mater. 16 (2004) 899–905.
[24] S.Z. Qiao, C.Z. Yu, Q.H. Hu, Y.G. Jin, X.F. Zhou, X.S. Zhao, G.Q. Lu, Micropor. Mesopor. Mater. 91 (2006) 59–69.
[25] C. Yu, B. Tian, J. Fan, G.D. Stucky, D. Zhao, Chem. Commun. 24 (2001) 2726–2727.
[26] W. Guo, J. Park, M.K. Oh, H. Jeong, W. Cho, Il. Kim, C.S. Ha, Chem. Mater. 15 (2003) 2295–2298.
[27] X.S. Zhao, G.Q. Lu, J. Phys. Chem. B 102 (1998) 1556–1561.
[28] R.S. Robert, A. Rafael, J.A. Dumesic, T.W. Root, Micropor. Mesopor. Mater. 66 (2003) 53–67.
[29] L.R. Snyder, J.W. Ward, J. Phys. Chem. 70 (1966) 3941–3952.
[30] S. Haukka, A. Root, J. Phys. Chem. 98 (1994) 1695–1703.
[31] R. Anwander, I. Nagl, M. Widenmeyer, J. Phys. Chem. B. 104 (2000) 3532–3544.
[32] J. Bu, H.-K. Rhee, Catal. Lett. 65 (2000) 141–145.
[33] Q. Tang, N. Yu, Z. Li, D. Wu, Y. Sun, Stud. Surf. Sci. Catal. 156 (2005) 649–655.
[34] P. Horcajada, A. Ramila, J. Perez-Pariente, M. Vallet-Regi, Micropor. Mesopor. Mater. 68 (2004) 105–109.
[35] J.M. Rosenholm, T. Czuryszkiewicz, F. Kleitz, J.B. Rosenholm, M. Lindén, Langmuir 23 (2007) 4315–4323.
[36] L. Zhong, K.C. Yeh, J. Pharm. Biomed. 16 (1998) 1051–1057.
[37] N. Nishiyama, D.-H. Park, Y. Egashira, K. Ueyama, Sep. Purif. Technol. 32 (2003) 127–132.
[38] J. Andersson, J. Rosenholm, S. Areva, M. Linden, Chem. Mater. 16 (2004) 4160–4167.